EBioMedicine 46 (2019) 119–132

Contents lists available at ScienceDirect

EBioMedicine

journal homepage: www.ebiomedicine.com

EBioMedicine
Published by THE LANCET

Research paper

Hepatectomy promotes recurrence of liver cancer by enhancing IL-11-STAT3 signaling

Dongyao Wang [a,b], Xiaohu Zheng [a,b], Binqing Fu [a,b], Zhigang Nian [a,b], Yeben Qian [c], Rui Sun [a,b], Zhigang Tian [a,b,*], Haiming Wei [a,b,*]

[a] Division of Molecular Medicine, Hefei National Laboratory for Physical Sciences at Microscale, The CAS Key Laboratory of Innate Immunity and Chronic Disease, School of Life Sciences, University of Science and Technology of China, Hefei, Anhui 230027, China
[b] Institute of Immunology, University of Science and Technology of China, Hefei, Anhui 230027, China
[c] Department of General Surgery, First Affiliated Hospital of Anhui Medical University, Hefei, Anhui 230027, China

ARTICLE INFO

Article history:
Received 27 March 2019
Received in revised form 18 July 2019
Accepted 22 July 2019
Available online 30 July 2019

Keywords:
Hepatocellular carcinoma
Surgical resection
IL-11-STAT3 signaling
Recurrence
Napabucasin

ABSTRACT

Background: Patients undergoing surgical resection of hepatocellular carcinoma (HCC) are at risk of recurrence; however, the underlying mechanism remains poorly understood.
Methods: Through the analysis of gene expression profiles in tumour and matched normal tissues from patients with hepatocellular carcinoma (HCC), we identified differences in interleukin-11 (*IL-11*) expression. Further, we used genetic mouse, orthotopic tumour, chemically induced, and orthotopic allograft models to study the correlation between IL-11 and postsurgical recurrence. Additionally, we conducted a series of experiments, including histology and immunohistochemistry analysis, three-dimensional culture, immunofluorescence, western blotting, enzyme-linked immunosorbent assay (ELISA) and flow cytometry to investigate the role of IL-11-signal transducer and activator of transcription 3 (STAT3) signaling in HCC recurrence.
Findings: We demonstrate that IL-11 levels increase after surgery, triggering HCC outgrowth. Accordingly, pharmacological blocking of IL-11-STAT3 signaling in model systems significantly alleviates tumour cell proliferation and suppresses postsurgical recurrence of HCC tumours.
Interpretation: These data demonstrate that IL-11 has a central role in postsurgical HCC recurrence, and that inhibition of IL-11-STAT3 signaling is a potential therapeutic strategy to prevent recurrence.
Fund: Natural Science Foundation of China.

1. Introduction

Primary liver cancer is a major public health problem. It is the sixth most common cancer worldwide and the second leading cause of cancer-related mortality, responsible for almost 800,000 deaths per year [1,2]. Hepatocellular carcinoma (HCC) is the most common histologic type of liver cancer, currently representing 85%–90% of cases [3,4]. Effective therapy for HCC remains a major challenge, as the tumours are chemotherapy resistant and, owing to an inadequate understanding of its genomic traits and molecular characteristics, the disease is generally diagnosed at an advanced stage. Surgical resection remains the most effective treatment and is widely recommended [5].

The high recurrence rate remains the most serious challenge for surgical resection, and the five-year survival rate is only 30%–40% [6]. Although >70% of patients with HCC experience recurrence after several years, a substantial fraction (approximately 20%) experience recurrence within six months after surgical resection. Moreover, the mechanism underlying postsurgical recurrence and, therefore, means to prevent it, remain unresolved [7].

Other than tumour characteristics, the onset and progression of HCC recurrence may be facilitated by complex interactions between inflammation levels and immune reactions, and several studies have attempted to uncover the mechanisms underpinning this process [8,9]. Weinberg et al. demonstrated that the outgrowth of distant metastases could be triggered by surgery and the wound-healing response, mediated by myeloid cells in particular. In addition, treatment with the anti-inflammatory drug, meloxicam, can attenuate surgery-induced tumour outgrowth [10]. The liver is an organ with special properties, including robust regeneration ability. Recurrence is often detected in *in situ* following surgical resection of liver tumours. In addition, numerous inflammatory cytokines, including members of the interleukin (IL)-6 family, which is defined by shared use of the gp130 receptor β-subunit (*e.g.*, IL-6 and IL-11), contribute

* Corresponding authors at: School of Life Sciences, University of Science and Technology of China, 443 Huangshan Road, Hefei city 230027, Anhui, China.
E-mail addresses: tzg@ustc.edu.cn (Z. Tian), ustcwhm@ustc.edu.cn (H. Wei).

https://doi.org/10.1016/j.ebiom.2019.07.058

Research in context

Evidence before this study

Hepatocellular carcinoma (HCC) is a major public health problem worldwide, and the incidence of HCC and associated mortality are increasing. Owing to an inadequate understanding of its molecular characteristics and chemotherapy resistance, HCC is almost always diagnosed at an advanced stage. Surgical resection is a widely recommended treatment for HCC; however, recurrence is often detected in *in situ*. Liver has robust regeneration ability, and previous studies have demonstrated that IL-11, a member of the IL-6 family, contributes to wound healing and hepatocyte compensatory proliferation. Thus, we hypothesised that IL-11 may play a role in both liver regeneration and HCC recurrence.

Added value of this study

We found that IL-11 expression was significantly up-regulated in HCC by microarray and TCGA database analyses, and that IL-11 protein levels increased after surgical resection. Additionally, IL-11-STAT3 signaling could trigger tumour outgrowth. Further, genetic ablation of Il6 did not significantly reduce the tumour burden in mice that had undergone hepatectomy. Moreover, inhibition of IL-11-STAT3 signaling in different HCC models markedly prevented tumour outgrowth and postsurgical recurrence.

Implications of all the available evidence

This study suggests that IL-11 is a potent driver of postsurgical recurrence in patients with HCC, and that the pharmacologic inhibition of IL-11-STAT3 signaling prevents postsurgical recurrence.

to wound healing and hepatocyte proliferation, and are also associated with cancer development after surgery [11]. Hence, much research has focused on IL-6, and IL-6 signaling has been documented in neoplastic epithelial cells and studied in clinical trials of treatments for renal, ovarian, breast, and prostate cancers [12–16]. Here, we demonstrate the role of the related cytokine, IL-11, in postsurgical recurrence of HCC.

During the wound healing response, IL-11 expression is induced by cyclo-oxygenase 2 in breast cancer cells and appears to be required for osteolytic bone metastases [17,18]. IL-11 is also verified as a key cytokine involved in gastrointestinal tumourigenesis and can be targeted therapeutically [18–20]. Signal transducer and activator of transcription factor 3 (STAT3) is an important transcription factor that is activated by IL-6 and IL-11, and involved in inflammation, oncogenesis, proliferation, and survival [16,21]. Excessive STAT3 activation is a characteristic of the majority of solid cancers [22,23], and hepatocyte-specific inhibition of STAT3 can reverse chemically- induced HCC in a mouse model, suggesting that targeting STAT3 signaling may confer significant therapeutic benefits in these malignancies [24].

Whether therapeutic inhibition of IL-11-STAT3 signaling can prevent HCC recurrence after surgical resection has yet to be addressed. Therefore, we designed several murine model systems to demonstrate that IL-11 has a crucial role in linking compensatory proliferation with recurrence after surgical resection and that pharmacologic inhibition of IL-11-STAT3 signaling attenuates recurrence. Our results suggest that this effective and inexpensive treatment may improve clinical outcomes for patients with HCC.

2. Materials and methods

2.1. Clinical samples

Fresh tumour and adjacent tissue samples were prospectively obtained from patients with HCC undergoing surgery at the Department of General Surgery of Anhui Provincial Hospital (Hefei, Anhui, China). The details of all patients involved in this study are provided in Supplementary Table S1. The collection of all samples was in accordance with the ethical guidelines of the 1975 Declaration of Helsinki, the Principles of Good Clinical Practice, and the guidelines of China's regulatory requirements, and was approved by the ethical review board of the University of Science and Technology of China (No. USTCEC201600004). Each provided written For Peer Review informed consent.

2.2. Mice

Male C57BL/6 wide type mice (WT; 2 weeks and 6 weeks old) were purchased from the Shanghai Experimental Animal Center of the Chinese Academy of Science (Shanghai, China). The $Il6^{KO}$ mice were a generous gift from Prof. Zhexiong Lian (South China University of Technology, China). All animals were kept under specific pathogen-free conditions. All of the experimental procedures involving animals were conducted in accordance with the National Guidelines for Animal Usage in Research (China) and permission for these animal studies was obtained from the Ethics Committee at the University of Science & Technology of China.

2.3. Generation of the $Il\text{-}11r\alpha^{KO}$ mice

$Il\text{-}11r\alpha^{KO}$ mice were generated using CRISPR-Cas9 technology, according to previous reports [23,25], and sgRNA was designed to specifically target the *Il-11rα* gene. Paired sgRNA oligos were then designed using tools from the Zhang Lab, at MIT (http://crispr.mit.edu/), and BLAST or BLAT searches of the UCSC or ENSEMBL genome databases using sgRNA target sites conducted to identify sequences with few or no related sites in the genome. Next, oligonucleotides were synthesized, annealed, and inserted into the sgRNA expression vector (pUC57-sgRNA plasmid Addgene 51,132). Paired sgRNA plasmids were then digested with *Dra*I and purified using a MinElute PCR Purification kit (QIAGEN, 28004). *In vitro* transcription of the sgRNAs was performed using a MEGA-short-script kit (Ambion, AM1354), and a MEGA clear kit (Ambion, AM1908) was used to purify the sgRNAs, according to the manufacturer's instructions [26]. We digested the Cas9 plasmid, pST1374-NLS-flag-linker-Cas9 (Addgene44758) using *Age*I, purified the product *in vitro*, and transcribed Cas9 with an mMESSAGEmMACHINET7 Ultra kit (Ambion, AM1345), according to the manufacturer's instructions. Cas9 mRNA was then purified using an RNeasy Mini kit (QIAGEN, 74104). Yields of *Cas9* mRNA and sgRNA were assessed with a One-Drop OD-1000+ spectrophotometer. C57BL/6 J mouse zygotes were superovulated by injection with pregnant mare serum gonadotropin (5 IU/100 ml) and human chorionic gonadotropin (5 IU/100 ml). We used DEPC-treated water to dilute *Cas9* mRNA to a final concentration of 20 ng/ml and the sgRNAs (5 ng/ml) in a final volume of 50 ml. Microinjection and embryo transfer were performed using standard methods to generate transgenic mice, as previously described [26]. We injected the RNA mixture into both the cytoplasm and the larger (male) pronucleus. The genotype and phenotype of the genetically ablated mice were analyzed by sequencing of the target genome segment and flow cytometry (FCM) (Supplementary Fig. 3).

2.4. Cell lines

All cell lines were tested negative for mycoplasma contamination by PCR. Hepa1–6 cells were obtained directly from the Shanghai Cell Bank

(Chinese Academy of Sciences, Shanghai, China) and cultured in complete Dulbecco's minimum essential medium (DMEM) (HyClone, Logan, UT, U.S.A.) supplemented with 10% fetal bovine serum (GIBCO, Grand Island, NY, U.S.A.), plus 1% streptomycin and penicillin at 37 °C and 5% CO2.

2.5. Interleukin (IL) measurement by enzyme-linked immunosorbent assay (ELISA)

Liver tissues were homogenised in cell lysis buffer on ice, then centrifuged at 16,000*g* for 10 min, and supernatants collected. Concentrations of IL-6 and IL-11 were measured using mouse IL-6 and IL-11 ELISA kits, according to the manufacturer's instructions.

2.6. Establishment of the HCC model and napabucasin treatment

A diethylnitrosamine (DEN)-induced HCC model was constructed by administering a single intraperitoneal injection of DEN (Sigma-Aldrich, # N0258) to 14-day-old male mice. Eight months later, tumours were harvested and cut into 2 × 2 mm pieces, then the fresh tumour tissues were subcutaneously injected into the right flanks of WT mice to stabilise the tumours. When tumours reached 1 × 1 cm, they were cut into 1 × 1 mm fragments and directly injected into the livers of WT mice. Other HCC models were constructed by administering a single intrahepatic injection of Hepa1–6 cells (1·5 × 10 [6]/20 μl) or a single intra-splenic injection of Hepa1–6 cells (1·5 × 10 [6]/50 μl or 2·0 × 10 [6]/50 μl) into male C57BL/6 mice. To study recurrence, tumours were observed two weeks later through the opened abdominal cavity. Then, tumours were resected with an electrosurgical knife, followed by intraperitoneal injection of phosphate-buffered saline (PBS) (controls) or napabucasin (40 mg/kg) twice per week. Finally, all mice were sacrificed at the specified time points.

2.7. Magnetic resonance imaging (MRI)

MRI experiments were performed on a 14·1-Tesla, 8·9-cm wide-bore, actively screened, vertical-bore MR spectrometer (Bruker Biospin, Germany). T1-weighted images were obtained using a two-dimensional modified driven equilibrium Fourier transform pulse sequence. Part of the work was performed using the Steady High Magnetic Field Facilities, High Magnetic Field Laboratory, CAS [27,28].

2.8. Histology and immunohistochemistry analyses

All tissues were first fixed in 12% neutral buffered formalin for standard histological processing. Six-micrometre-thick sections were carefully cut and stained with haematoxylin and eosin (HE), Sirius red (SR), or Mason's Trichrome. For immunohistochemistry analysis, tissues were de-paraffinised, then heat-induced antigen unmasking conducted. Immunohistochemical stains were performed with antibodies against proliferating cell nuclear antigen (PCNA; CST, # 2586; RRID: AB_2160343), CD31 (CST, # 77699; RRID: AB_2722705), AFP (abcam, # ab213328), IL-11 (SANTA CRUZ, # sc-133,063; RRID: AB_2125634), mice IL-11Rα (SANTA CRUZ, # sc-130,920; RRID: AB_2123736), human IL-11Rα (abcam, # ab125015; RRID: AB_10975018) and Phospho-STAT3 (Tyr705) (CST, # 9145; RRID: AB_2491009). Images were then taken with an OLYMPUS microscope. To further assess the immunostaining quantification, the slides were analyzed by an image analysis workstation (Image Pro Plus 6.0, Media Cybernetics).

2.9. Immunofluorescence analysis

For immunofluorescence analysis, Hepa1–6 cells were first stimulated with IL-6 (Peprotech, # 96–216–16-10) or IL-11 (Peprotech, # 96–220–11-10) for 32 h, with or without the STAT3 inhibitor, napabucasin (MedChem Express, # HY-13919), as indicated in the figure legends. Then, cells were fixed with 4% PFA and incubated in blocking buffer (5% goat serum with 0.5% Triton-X in PBS) at room temperature for 1 h. Cells were then collected and stained with PCNA antibody, followed by Alexa Fluor 594-conjugated goat anti-rat IgG (Invitrogen; # A-21247; RRID: AB_141778). Finally, cells were stained with DAPI. Images were visualised on a Zeiss 880 Meta multi-photon confocal microscope (Zeiss, Oberkochen, Germany).

2.10. Western blotting

After stimulation with murine IL-6 or IL-11 (50 or 100 ng/ml) for 30 min, Hepa1–6 cells were lysed in RIPA buffer containing proteinase inhibitors. Western blotting was performed according to standard protocols. Briefly, 50 μg protein samples were loaded and separated using sodium dodecyl sulphate polyacrylamide gel electrophoresis, before being transferred onto a 0·45 μm polyvinylidene fluoride membrane, blocked in 5% (w/v) bovine serum albumin, and incubated with primary antibodies. The following antibodies were used: STAT3 (CST, # 9139; RRID: AB_331757), Phospho-STAT3 (Tyr705) (CST, # 9131; RRID: AB_331586), horseradish peroxidase (HRP)-conjugated Goat Anti-Rabbit IgG, and HRP-conjugated Goat Anti-Rabbit IgG (Sangon Biotech, # D110087). Finally, protein bands were visualised and analyzed by chemiluminescence (Millipore).

2.11. Reverse transcription PCR

Total RNA was isolated from tissues using TRIzol (Invitrogen, # 15596026), according to the manufacturer's instructions. RNA concentration and quality were then determined by measuring light absorbance at 260 nm (A260) and the A260/A280 ratio, respectively. RNA was then reverse transcribed into cDNA using Moloney murine leukaemia virus reverse transcriptase and random primers. Primers are listed in Table S2.

2.12. Three-dimensional (3D) culture

For 3D cell culture, Hepa1–6 cells were seeded, at a density of 0·05 × 10^6 /ml, in medium mixed with hydrogel (NISSAN CHEMICAL INDUSTRIES, LTD.) according to the manufacturer's instructions. Cells were treated with IL-11 and incubated for 32 h, with or without napabucasin, under the indicated conditions. The seeding density was 0·05 × 10^6 /ml.

2.13. Microarray expression analysis

Microarray analyses were performed to determine the molecular signatures of tumour and matched normal tissues, using a whole human genome oligo microarray (Agilent, G4112F). Microarray image analysis and hierarchical clustering were performed as previously described [28].

2.14. Flow cytometry

Cells were labelled with fluorochrome-conjugated antibodies, 7-AAD (BD Bioscience, #559925), Annexin V (BD Bioscience, #556419; RRID: AB_2665412) or IL-11Rα (Santa Cruz, #sc-130,920; RRID: AB_2123736). Stained cells were detected on an LSR II flow cytometer (BD Biosciences) and analyzed with FlowJo software (Tree Star). Specific fluorescence indices were calculated as follows: median fluorescence of the respective specific mAb/median fluorescence of the isotype control.

2.15. Small interfering RNA transfection

Small interfering RNAs against IL-11Rα were synthesized by GenePharma. The small interfering RNAs targeted sequences were as

follows: 5′-GCCUACUGGAUGUGAGAUUTT-3′ (*Il-11rα*$^{\#1}$); 5′-GGAGGA GGUGAUAACAGAUTT-3′ (*Il-11rα*$^{\#2}$); and 5'-UUCUCCGAACGUGUCA CGUTT-3′ (mock). The small interfering RNAs were transfected into Hepa1–6 cells, using the Lipofectamine 2000 Reagent (Invitrogen), according to the manufacturer's instructions. Experiments were performed 24 h after transfection.

2.16. Statistical analysis

GraphPad Prism 6·0 software was used to perform statistical analyses. Differences between two groups were determined by two-tailed *t*-tests. No particular methods were used to determine whether the data met assumptions of the statistical approach. $P < 0·05$ was considered significant.

3. Results

3.1. HCC recurs after surgical resection

As the postsurgical recurrence rate of HCC is high [2,9,29–35], and given the large numbers of patients with HCC, we focused on the mechanisms underlying postsurgical recurrence. To demonstrate that HCC can recur in mice, we established a surgical orthotopic HCC resection model by implanting Hepa1–6 cells into the livers of recipient mice. After 2 weeks, we used an electrosurgical knife to resect the tumours, and detected postsurgical recurrence 7 days later, as described previously [36]. Pathologic analysis revealed that the tumours were clearly defined, and Sirius red (SR) staining revealed severe fibrosis following surgical resection (Fig. 1a and b). Further, after surgical resection, tumours also expressed higher levels of the angiogenesis marker, CD31, and the proliferation marker, PCNA (Fig. 1c–f), suggesting the substantial angiogenesis and proliferation. In summary, after surgical resection of HCC, postsurgical recurrence was frequently observed and accompanied by tumour proliferation.

3.2. Surgical wounding triggers HCC outgrowth

Given the recurrence of HCC and its rapid regeneration after surgery, and the fact that these tumours tend to recur *in situ*, we hypothesised that surgical resection both induces liver generation and promotes tumour outgrowth. Therefore, we used an experimental strategy, in which mouse livers were wounded by perforation or hepatectomy before the injection of tumour cells. Following perforation or resection of the left lateral lobe of the liver, we transferred Hepa1–6 cells by intrasplenic injection (Fig. 2a). Strikingly, pathologic analysis revealed that, after wounding or resection, reparative responses were significant drivers of tumour development and increased fibrosis (Fig. 2b and c). When invasive regions of tumours were scored separately, we found larger PCNA-positive and CD31-positive areas after surgery, suggesting that larger tumours were present in groups that had undergone surgical wounding (Fig. 2d–f). Furthermore, to directly assess whether tumour lesions were aggregated *in vivo* following hepatectomy, mice were subjected to ultra-high field magnetic resonance imaging (MRI). The results showed that mechanical injury significantly promoted tumour outgrowth and the normalised grayscale values of primary tumour lesions, regardless of whether tumour cells were implanted from the spleen or orthotopically implanted into the liver (Fig. 2g and h).

Next, to compare the growth rate of HCC during and after hepatectomy (during and after the liver regeneration phase), we established a mouse model to compare mice undergoing partial hepatectomy eight

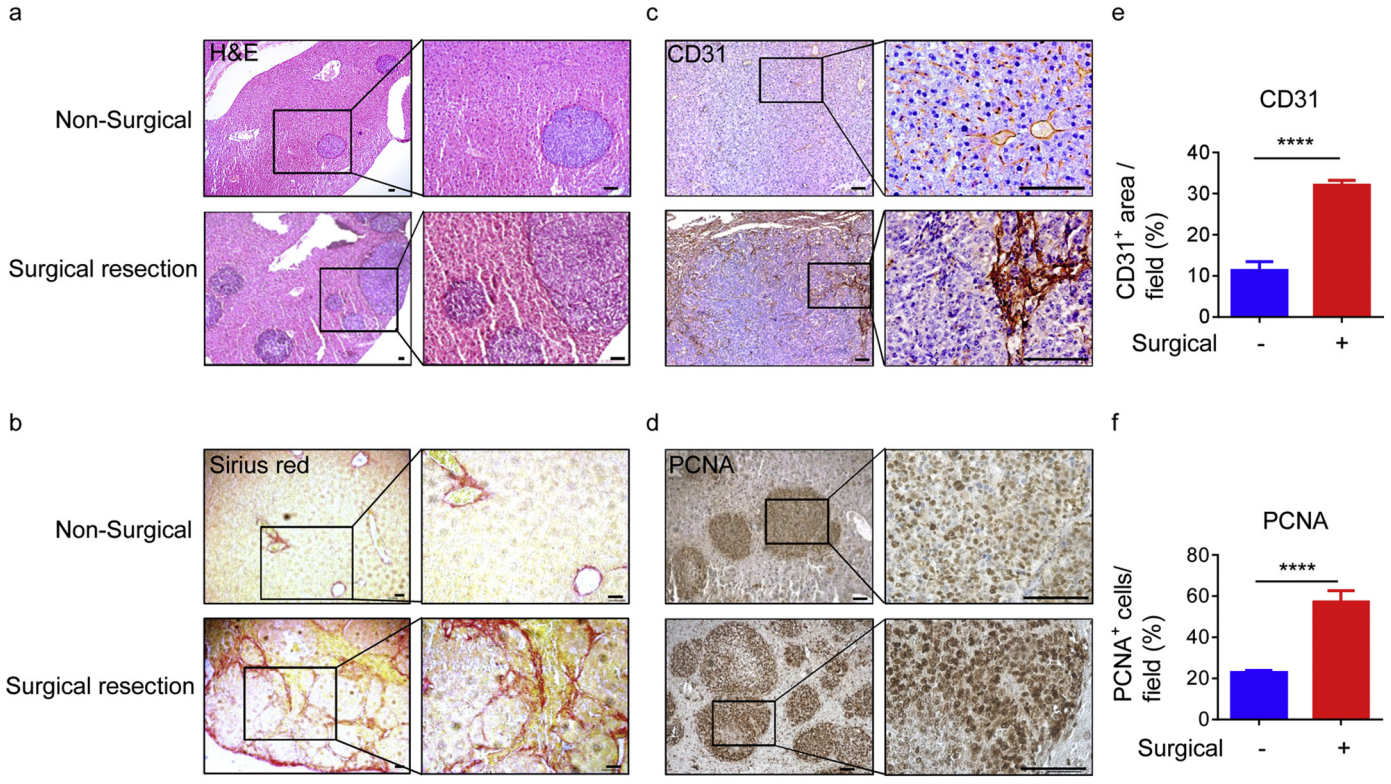

Fig. 1. HCC recurs after surgical resection. (a and b) The livers of 6-week-old male wild-type (WT) mice were injected with Hepa1–6 cells ($1·5 \times 10$ [6]), and an electrosurgical knife used to resect tumours two weeks later. Livers were then processed for histological monitoring after one week. Representative histology of the HE (a) and Sirius Red (SR) (b) stained sections from livers of the indicated mice. Data are representative of three independent experiments. Scale bars, 100 μm. (c and d) Representative images of IHC staining of CD31 (c) and PCNA (d) in liver samples from the indicated mice. Data are representative of three independent experiments. Scale bars, 100 μm. (e and f) Quantitation of the CD31-positive area per field (e) and PCNA-positive cells per field (f) in the harvested regions. Quantification was conducted by counting random fields (20 ×) in mouse liver sections. Surgical resection (red) and non-surgical (blue) tumours (four mice per group) were counted. Data are presented as mean ± SD. $^{****}p < 0·0001$ (unpaired Student's *t*-test).

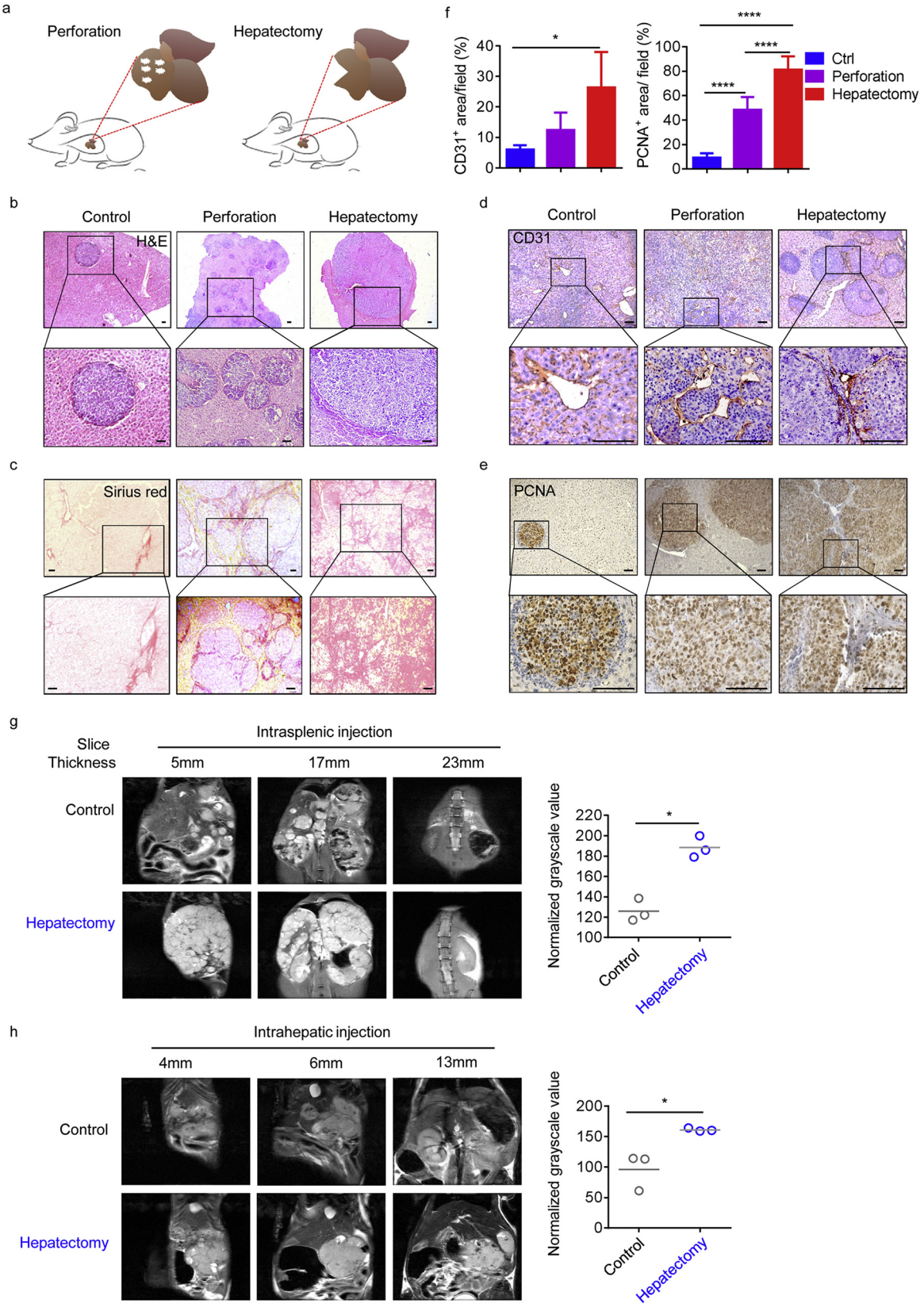

Fig. 2. Hepatectomy induces HCC outgrowth. (a) Schematic illustrating the experimental design Hepa1–6 cells ($1{\cdot}5 \times 10$ [6]) were injected into the spleens of mice that had previously been perforated at five points using a needle ($0{\cdot}6 \times 32$ mm), or had undergone resection of the left lateral lobe of the liver. (b and c) Representative histology of HE-stained (b) and SR-stained (c) liver samples from WT mice treated as illustrated in (a). Data are representative of three independent experiments. Scale bars, 100 μm. (d and e) Representative images of IHC staining for CD31 (d) and PCNA (e) in representative mouse liver samples. Data are representative of three independent experiments. Scale bars, 100 μm. (f) Quantitation of CD31-positive area per field (left), conducted by counting random fields (20 ×); and PCNA-positive cells per field (right), conducted by counting random fields (10 ×), in the harvested regions. Tumour samples from four mice in each group were counted. Data are presented as mean ± SD. $^{*}p < 0{\cdot}05$, $^{****}p < 0{\cdot}0001$ (unpaired Student's *t*-test). (g and h) Different MRI scan levels of representative mice from each treatment group. Left lateral liver lobes were resected from 50% of animals, then tumour cells injected from the spleen (g) or orthotopically from the liver (h). Graphs on the right show the mean normalised grayscale values at different slice thicknesses for (g) or (h), confirming their significance; $^{*}p < 0{\cdot}05$ (paired Student's *t*-test), $n = 3$; Data are presented as mean ± SD.

days before transferring tumour cells by intra-splenic injection ("after hepatectomy" group), with those undergoing partial hepatectomy and immediate transfer of Hepa1–6 cells ("hepatectomy" group) (Supplementary Fig. 1a). Strikingly, tumour-bearing mice in the "hepatectomy" group displayed a significantly greater increase in tumour burden, liver weight, and liver weight growth than the "after hepatectomy" group (Supplementary Fig. 1b and c). Further, we observed more and larger tumour nodules, and higher PCNA levels during (hepatectomy) than after (after hepatectomy) the regeneration phase (Supplementary Fig. 1 d to g), indicating that tumours became more aggressive during the regeneration phase. Taken together, these results suggest that surgery can induce HCC outgrowth.

3.3. IL-11 is overexpressed following hepatectomy

After surgical resection of HCC, inflammatory cytokines, including those of the IL-6 family, contribute to hepatocyte proliferation and wound healing, which are also associated with cancer development. To further explore the mechanisms underlying these observations, we initially used an oligonucleotide microarray and identified significant differences in gene expression profiles between tumours and paired adjacent tissues from patients with primary HCC who underwent surgical resection. Specifically, we identified target genes whose expression levels were up-regulated at least two fold ($P < 0{\cdot}01$) in tumour tissues compared with adjacent tissues. Then we divided target genes into several categories, including the interleukin family, interleukin receptor family, growth factor-related family, C-X-C motif chemokine ligand (CXCL) family, C-X-C motif chemokine receptor (CXCR) and C-C motif chemokine receptor (CCR) families (Fig. 3a).

Interestingly, *AFP* and *IL-11*, a dominant IL-6 family cytokine in gastrointestinal cancers [10,33], were highly expressed and significantly up-regulated in tumours compared with adjacent tissues. However, other genes such as *CCR4*, a potential diagnostic and prognostic marker in HCC [37], *CCR8*, *CXCL1*, and *IL-6Rα* seemed not significantly up-regulated or highly expressed in tumours. Using IHC staining, we found that IL-11 expression was significantly increased in tumour regions in patients with HCC (Fig. 3b and c), whereas IL-11Rα was highly expressed in both tumour and adjacent normal tissue (Supplementary Fig. 2a and b). Moreover, after acute liver injury in mice, IL-11 is produced and released to induce STAT3 phosphorylation in healthy hepatocytes, thus mediating their proliferation [38]. Therefore, we hypothesised that IL-11 could play an important role in the liver microenvironment following surgery.

In the absence of a clinical control group of patients with HCC who had not undergone surgical treatment, we established another mouse model to determine whether IL-11 protein levels increased after surgical resection, by comparing mice undergoing partial hepatectomy with a control group undergoing a sham operation. By IHC, we showed that both IL-11 and IL-11Rα were elevated after surgery. IL-11 reached a maximum level on day 5 after hepatectomy (Fig. 3d and e), while the highest IL-11Rα expression levels were on day 7 (Supplementary Fig. 2c and d). Using ELISA, we also found that levels of IL-11 increased in liver tissue 5 days after resection (Fig. 3f). Together, these data imply that IL-11 levels do indeed increase during liver regeneration following hepatectomy.

3.4. IL-11 signaling drives HCC outgrowth after surgical resection

Given that hepatectomy could trigger HCC outgrowth concomitant with regeneration, and that IL-11 was overexpressed during this progression, we generated *Il-11rα*^{KO} mice to further explore the role of IL-11 signaling in postsurgical recurrence of HCC (Supplementary Fig. 3a and b). Consistent with the earlier experiments that focused on surgical resection, we established a surgical orthotopic HCC resection model. Mice were sacrificed 1 week after surgical resection of liver tumours, and we found tumours were almost completely absent at autopsy in the *Il-11rα*^{KO} mice, what's more, overall tumour numbers and burden were significantly reduced (Fig. 4a and b).

To ascertain whether tumourigenesis also decreased, we performed IHC analyses of the tumours and verified significant reductions in PCNA, AFP, and STAT3 Y705 phosphorylation (pTyr-STAT3) in *Il-11rα*^{KO} mice (Fig. 4c). These observations are consistent with our proposal that IL-11 signaling has a role in the promotion of HCC recurrence after surgical resection. Moreover, to our surprise, serum levels of IL-11 increased after surgery in wild-type (WT) mice, but not *Il-11rα*^{KO} mice on day 7; however, those of IL-6 did not (Fig. 4d). Collectively, our results confirm that IL-11 signaling is necessary for HCC recurrence after surgical resection.

3.5. Inhibition of IL-11 signaling induces tumour cell apoptosis in vitro

Furthermore, to determine whether blocking IL-11-IL-11Rα signaling could induce tumour cells apoptosis *in vitro*, Hepa1–6 cells were transfected with siRNA targeting *Il-11rα*, and then stimulated with/without IL-11 (Supplementary Fig. 4a and b). We found that *Il-11rα* silencing in these cells significantly increased the percentage of apoptosis, relative to controls, regardless of whether or not IL-11 was added (Supplementary Fig. 4c and e). In addition, we demonstrated that the mean fluorescence intensity (MFI) of PCNA staining was significantly decreased in cells transfected with siRNA targeting *Il-11rα*, irrespective of IL-11 supplementation (Supplementary Fig. 4d and f). These data showed that using siRNA to directly block IL-11-IL-11Rα signaling induced tumour cell apoptosis *in vitro*.

Having demonstrated that IL-11 is required for HCC recurrence after hepatectomy, and considering the study by Nishina et al., showing that IL-11-STAT3 signaling mediates proliferation of hepatocytes after acute liver injury in mice [38], we endeavoured to determine whether inhibition of IL-11-STAT3 signaling could also induce Hepa1–6 cell apoptosis *in vitro*. To maximally maintain the stereo-structural characteristics and functions of the cells as they are *in vivo*, we used a three dimensional (3D) culture system, and found that IL-11 promoted Hepa1–6 cells proliferation (Fig. 5a and b).

Next, to demonstrate whether inhibition of IL-11-STAT3 signaling obstructs cell proliferation, we used an inhibitor of STAT3 transcription, napabucasin, which can suppress cancer stemness. Napabucasin was approved as an orphan drug for pancreatic cancer [39] and is undergoing a clinical trial for treatment of advanced gastric and gastro-oesophageal junction cancer [40]. Initially, we simulated the *in vivo* environment after surgical resection, in which IL-11 was highly expressed; following the addition of napabucasin, we found less globular cell mass (Fig. 5a and b) and more 7-AAD^{+} cells (Fig. 5c and d). Using immunofluorescence, we observed reduced expression of PCNA in cells cultured with napabucasin, irrespective of whether they were supplemented with IL-11 (Fig. 5e and f). To further verify that napabucasin induced tumour cell apoptosis or death through down-regulation of STAT3 phosphorylation, we performed western blotting, which confirmed that levels of pTyr-STAT3 increased after stimulation with IL-11; however, treatment with napabucasin strongly inhibited pTyr-STAT3 levels (Fig. 5g).

These results indicate that IL-11-STAT3 signaling promotes the proliferation of tumour cells *in vitro*. Further suppression of this signaling using napabucasin significantly reduced tumour cell proliferation, implying that a similar effect could occur after surgical resection of HCC *in vivo*.

3.6. Inhibition of STAT3 phosphorylation prevents postsurgical recurrence

Given our finding that inhibition of STAT3 phosphorylation reduced tumour cell proliferation *in vitro*, we investigated whether treatment with napabucasin could attenuate HCC recurrence after surgery. In mice that had been orthotopically injected with Hepa1–6 cells, we

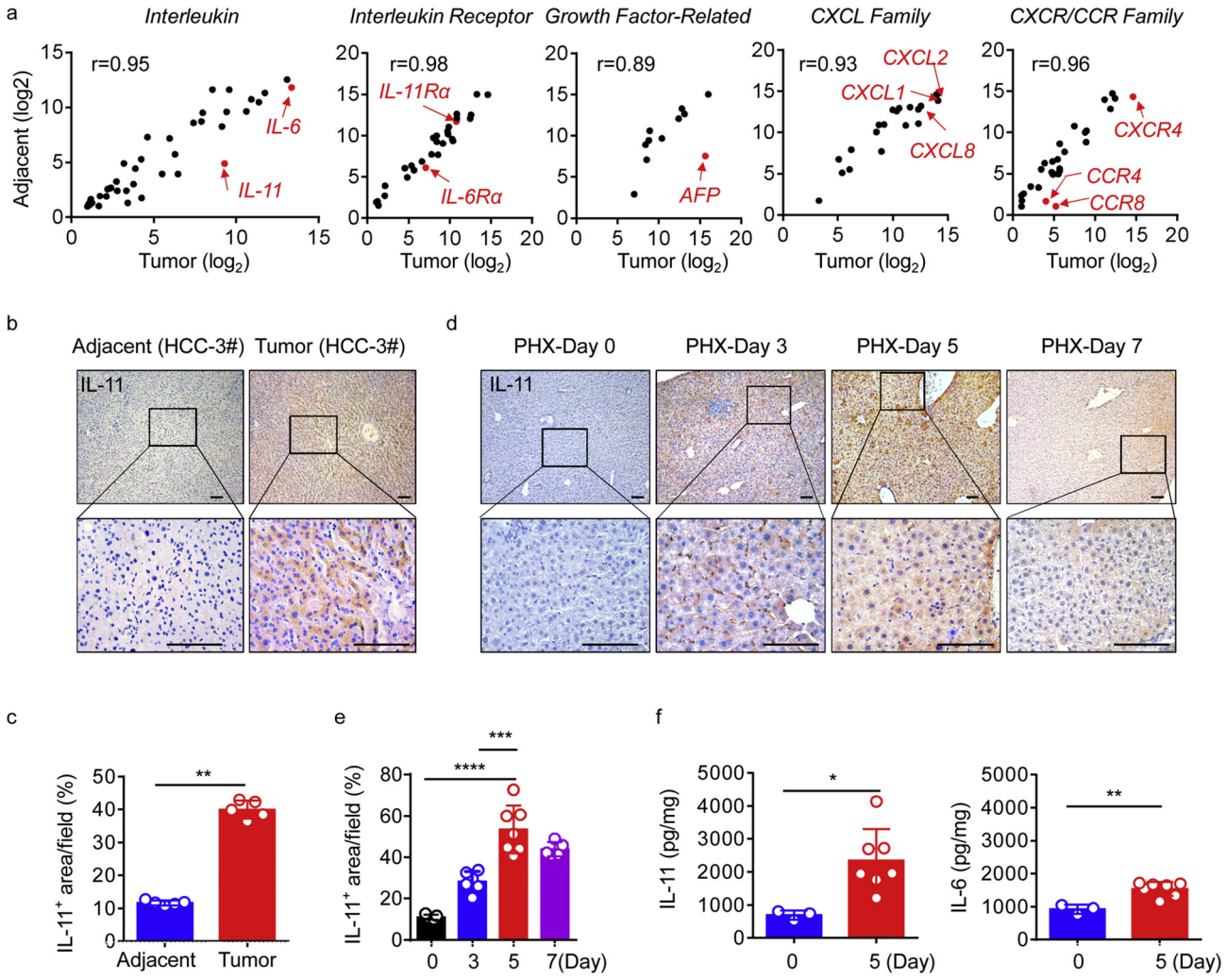

Fig. 3. IL-11 is overexpressed after surgery. (a) Whole-genome transcriptome analyses using microarrays. The scatter plot indicates genes belonging to different categories in tumour and matched adjacent liver tissue from patients with HCC. Data are presented as normalised $\log_2$ values, and several important genes, including *IL-11*, are indicated by red dots. R values represent the overall distribution of the central tendency. (b and c) Representative images of IHC staining of IL-11 (b) and quantification (c) in liver tumour tissue (red) and adjacent tissue (blue) of HCC patients. Scale bars, 100 μm. $^{**}p < 0{\cdot}01$ (paired Student's *t*-test) $n = 5$. (d and e) Representative images of IHC staining of IL-11 in the livers of 6-week-old male WT mice without injection of tumour cells at different time points after hepatectomy. Scale bars, 100 μm (d). $n = 5$–7. Data are presented as mean ± SD. $^{***}p < 0{\cdot}001$, $^{****}p < 0{\cdot}0001$ (unpaired Student's *t*-test) (e). (f) Total IL-6 and IL-11 levels in liver tissue from WT mice 5 days after hepatectomy, determined by ELISA. $n = 3$ for day 0 (blue), $n = 9$ for day 5 (red). Data are presented as mean ± SD. $^{*}p < 0{\cdot}05$, $^{**}p < 0{\cdot}01$ (unpaired Student's *t*-test).

found that tumour growth was significantly inhibited after administration of 40 mg/kg napabucasin (Fig. 6a and b). Napabucasin therapy reduced liver tumour burden, with an almost complete absence of tumours, minor pathological damage, and little tumour proliferation, compared with the control group (Fig. 6b and c).

Next we determined whether postsurgical recurrence could be prevented by napabucasin. Here, we relied on a well-established surgical orthotopic HCC resection mouse model, which we treated twice with napabucasin post-surgery (Fig. 6d). Notably, there was almost no tumour recurrence after treatment. Successful treatment with the STAT3 inhibitor was also associated with significant reductions in overall tumour numbers and burden, as well as decreased tumourigenesis (Fig. 6e–g). Moreover, considering that excessive STAT3 activation is a feature of most solid cancers, we assessed pTyr-STAT3 expression. High expression levels were observed in WT mice after surgery, and these were significantly reduced by napabucasin treatment (Supplementary Fig. 5).

Given the evidence that IL-6 plays an important part in HCC development [15,16,21,41,42], we used $Il6^{KO}$ mice to explore the effect of IL-6 on recurrence after surgery. Initially, we found that genetic ablation of *Il6* did not significantly reduce tumour numbers or burden in mice that underwent partial hepatectomy before the injection of Hepa1–6 cells (Fig. 7a and b). Pathologic and IHC analyses did not reveal any differences between $Il6^{KO}$ and WT mice, in terms of tumour growth or tumourigenesis (Fig. 7c). Using a surgical orthotopic HCC resection model, we also found that HCC recurred in postsurgical $Il6^{KO}$ mice, and that treatment with napabucasin successfully prevented recurrence, with decreased PCNA expression (Fig. 7d-g). These results indicate that, although both IL-6 and IL-11 signaling accompany STAT3 activation in hepatocytes and contribute to inflammation after surgery, enhanced IL-11 signaling is responsible for the development of postsurgical recurrence. Collectively, our data suggest that repetitive administration of a STAT3 inhibitor after surgical resection can effectively inhibit tumour recurrence.

3.7. Blocking STAT3 phosphorylation inhibits IL-11-induced HCC outgrowth in vivo

Our initial experiments established that IL-11 is highly expressed in tumours and tissues after surgery, and that STAT3 inhibition efficiently

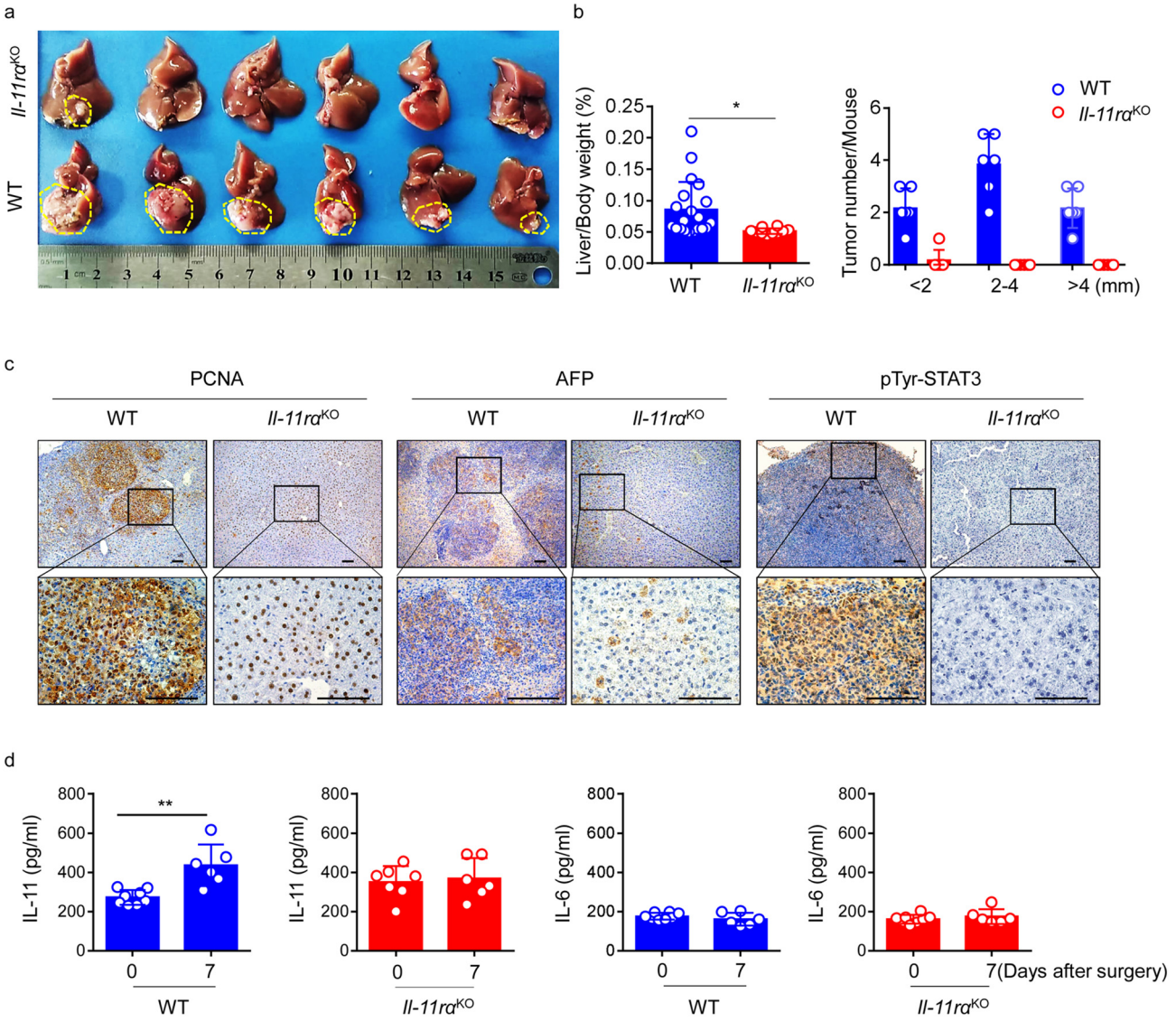

Fig. 4. IL-11 signaling is required for HCC outgrowth after surgical resection. (a) Livers of eight-week-old Il-11rαKO (top row) and WT (bottom row) mice were orthotopically injected with Hepa1–6 cells ($1{\cdot}5 \times 10$ [6]). After 2 weeks, tumours were surgically resected, and mice sacrificed 1 week later. Images are representative pictures of HCC tumours from the two groups, each n = 6. Data are representative of three independent experiments. Scale bar, 1 cm. (b) Ratio of liver weight to body weight (left) and liver tumour burden (right) were calculated in the indicated groups at autopsy. Horizontal lines refer to mean values. n = 10–20. Data were pooled from three independent experiments. $^{*}p < 0{\cdot}05$ (unpaired Student's t-test). (c) Representative PCNA (left), AFP (middle), and pTyr-STAT3 (right) IHC analysis of mouse liver samples after surgical tumour resection. Results are representative of three independent experiments. Scale bars, 100 μm. (d) IL-11 and IL-6 levels in serum from WT and Il-11rαKO mice at different time points after surgery determined by ELISA. The results are expressed as mean ± SEM. $^{**}p < 0{\cdot}01$ (unpaired Student's t-test). n ≥ 4 for each group.

prevented surgery-induced HCC recurrence. To mimic the environment of the liver after hepatectomy, and to directly assess IL-11 and STAT3 function in tumour growth, we orthotopically injected Hepa1–6 cells into mice, then injected IL-11 twice, along with napabucasin (Fig. 8a). Mice injected with IL-11 developed higher tumour burdens (Fig. 8b, c and Supplementary Fig. 6). After injection of IL-11, pathologic analysis revealed increased tumour areas. Severe fibrosis was detected by HE and Masson trichrome staining (Fig. 8d), accompanied by strong PCNA and AFP staining (Fig. 8e and f), suggesting that IL-11 is a potent trigger of proliferation and tumourigenesis; however, as expected, co-injection of IL-11 and napabucasin led to reduced tumour burden, minor pathologic damage, and little tumour proliferation (Fig. 8b–d). Consistent with these data, we also found significant decreases in PCNA and AFP expression (Fig. 8e and f).

To further demonstrate that inhibition of IL-11-STAT3 signaling could reduce recurrence in a spontaneous HCC model, we generated both chemically-induced and an orthotopic allograft models. First, we intraperitoneally injected DEN into 2-week-old male WT mice [43] (Supplementary Fig. 7a). Tumours were harvested after 8 months, and expression levels of IL-11 signaling-related genes determined by PCR. High levels of IL-11 protein were found in HCC tissue (Supplementary Fig. 7b and c), indicating that DEN-induced HCC also occurs *via* IL-11-STAT3 signaling-induced growth. To stabilise tumours, they were cut into pieces and subcutaneously injected into the right flanks of WT mice. When tumours reached 1×1 cm, they were cut into fragments and orthotopically injected into the livers of WT mice (Supplementary Fig. 7a). Four months later, tumour formation was evident (Supplementary Fig. 7d). As expected, postsurgical mice treated with napabucasin displayed significantly reduced recurrence in the orthotopic allograft model, accompanied by decreased expression of PCNA and pTyr-STAT3 (Supplementary Fig. 7e-g), demonstrating that therapeutic inhibition of STAT3 phosphorylation prevents IL-11-induced HCC outgrowth. Taken together, these results strongly support a non-redundant role for IL-11-STAT3-mediated signaling in postsurgical recurrence of HCC.

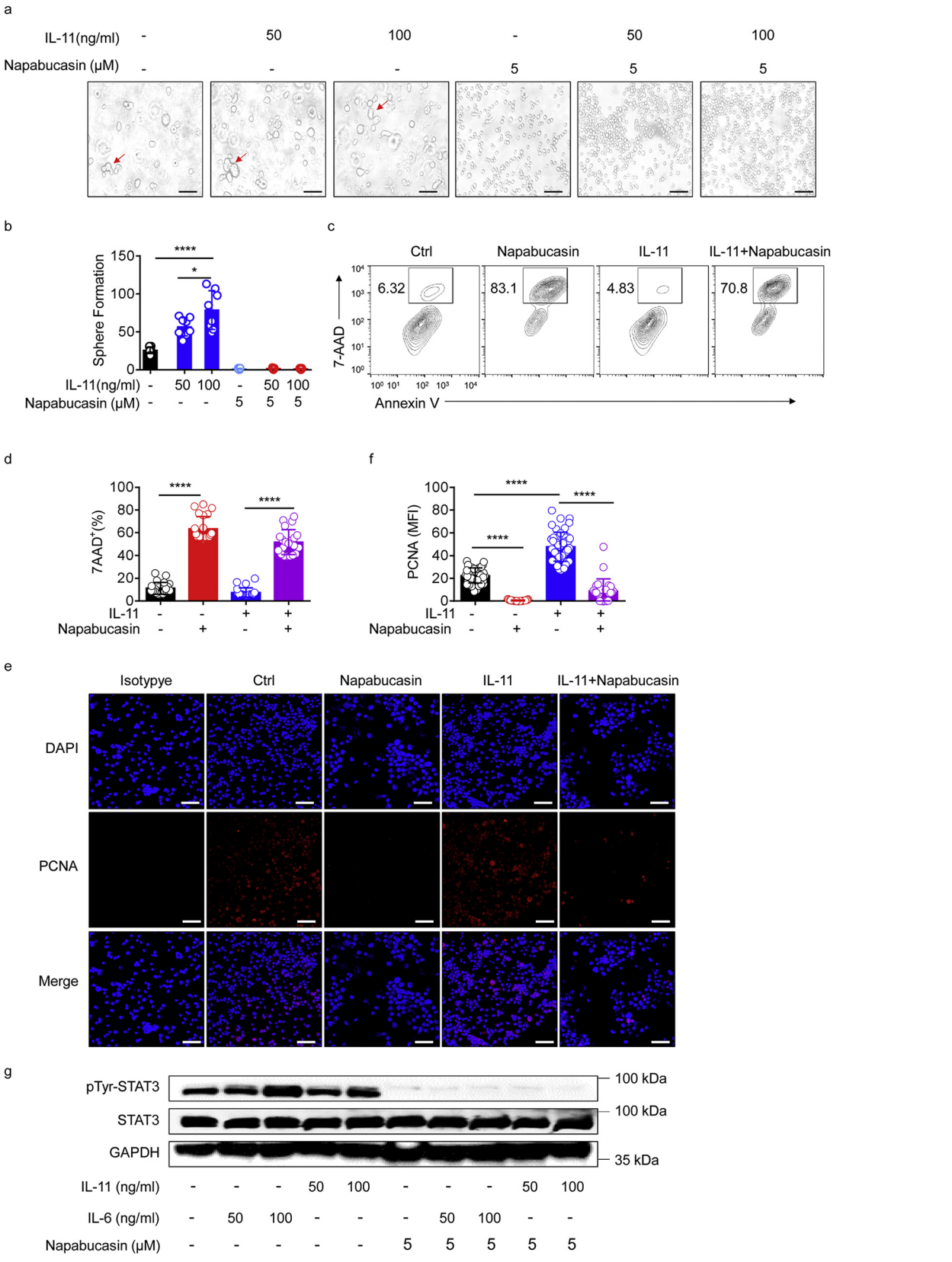

Fig. 5. Inhibition of IL-11 signaling promotes tumour cell apoptosis. (a) Representative bright-field images (×20 magnification) of globular cell mass formation in 3D cultures treated with IL-11 (50 or 100 ng/ml) and/or napabucasin (5 μM) for 32 h. Results are representative of two independent experiments. Scale bars, 100 μm. (b) Statistical analysis of globular cell mass counts at ×10 magnification. The results are expressed as mean ± SEM. $^{*}p < 0{\cdot}05$, $^{****}p < 0{\cdot}0001$ (unpaired Student's *t*-test). (c) Representative density plots showing apoptosis of Hepa1–6 cells by double staining with Annexin V and 7-AAD under the indicated culture conditions. (d) Statistical analysis of the percentage of 7-AAD^{+} Hepa1–6 cells after treatment. Data are representative of three independent experiments. The results are expressed as mean ± SEM. $^{****}p < 0{\cdot}0001$ (unpaired Student's *t*-test). (e) Immunofluorescence staining showing PCNA expression in Hepa1–6 cells cultured under the indicated conditions. Data are representative of three independent experiments. Scale bar, 100 μm. (f) Statistical analysis of mean fluorescence intensity (MFI) values for PCNA staining in Hepa1–6 cells treated under the indicated conditions. Data are representative of three independent experiments. $^{****}p < 0{\cdot}0001$ (unpaired Student's *t*-test). The results are expressed as mean ± SEM. (g) Representative immunoblot analysis for pTyr-STAT3 in Hep1–6 cell lysates after the indicated treatments. GAPDH was used as a control. Data are representative of six independent experiments.

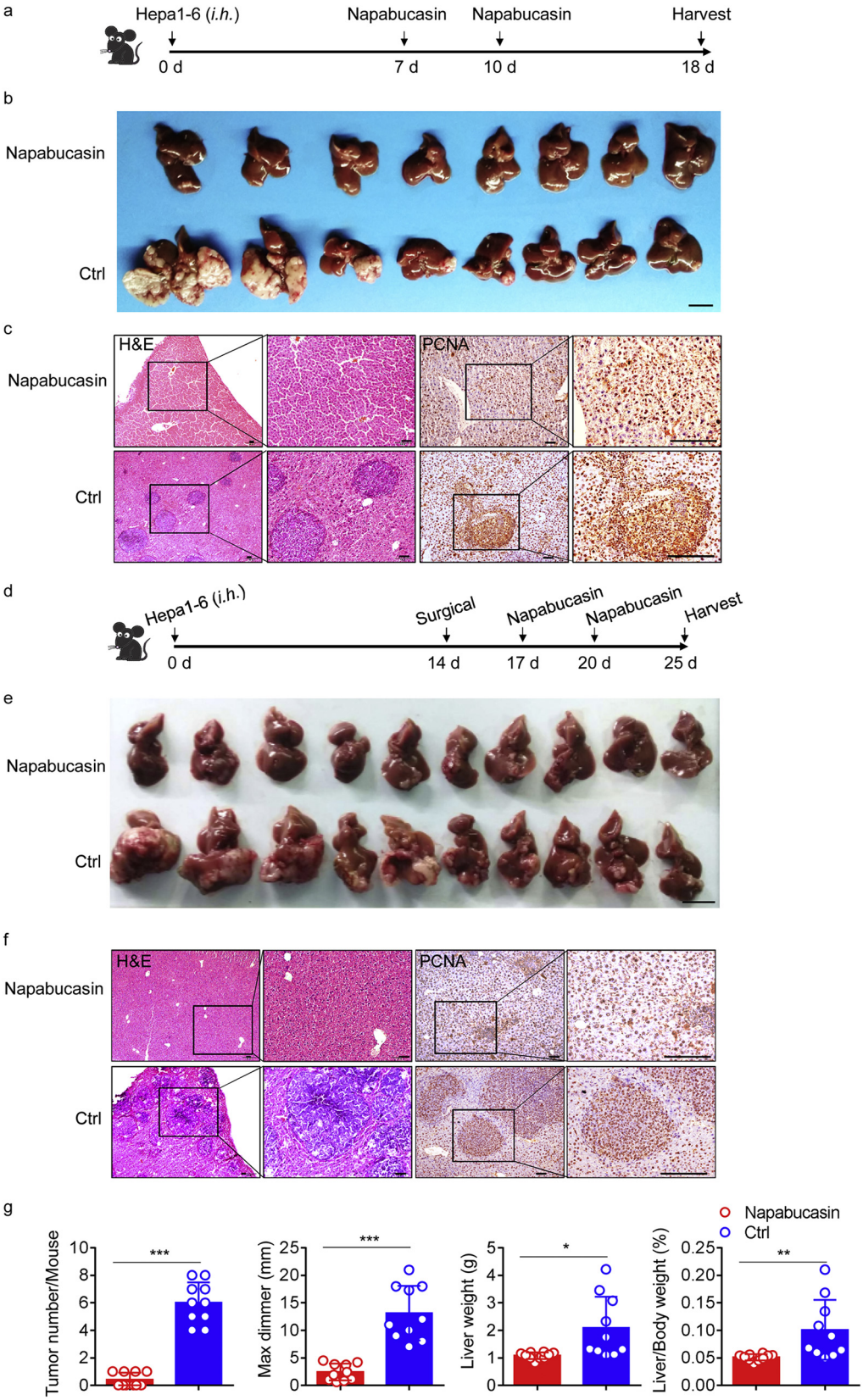

Fig. 6. Napabucasin can reduce postsurgical HCC recurrence. (a) Schematic representation of the HCC model. A single injection of Hepa1–6 cells ($1{\cdot}5 \times 10$ [6]) was administered into the livers of 8-week-old WT mice, followed by two doses of napabucasin (40 mg/kg) from day 7. (b) Representative pictures of HCC from the two groups on day 18; n = 8 for each group. Data are representative of two independent experiments. Scale bar, 1 cm. (c) Low-magnification HE staining (left) and IHC staining of PCNA (right) in mouse livers from the indicated groups. Data are representative of three independent experiments. Scale bars, 100 μm. (d) Schematic representation of the HCC recurrence model. A single injection of Hepa1–6 cells ($1{\cdot}5 \times 10$ [6]) was administered into the livers of mice; two weeks later, an electrosurgical knife was used to resect tumours, followed by two doses of napabucasin (40 mg/kg). (e) Representative pictures of HCC in the two groups on day 25, n = 10 for each group. Scale bar, 1 cm. (f) Representative images of HE and PCNA (IHC) staining in tumour sections from the indicated mice. Data are representative of three independent experiments. Scale bars, 100 μm. (g) HCC burden in individual mice from the indicated groups at autopsy on day 25. n ≥ 8 per group. The results are expressed as mean ± SEM. $^{*}p < 0{\cdot}05$, $^{**}p < 0{\cdot}01$, $^{***}p < 0{\cdot}001$ (unpaired Student's t-test).

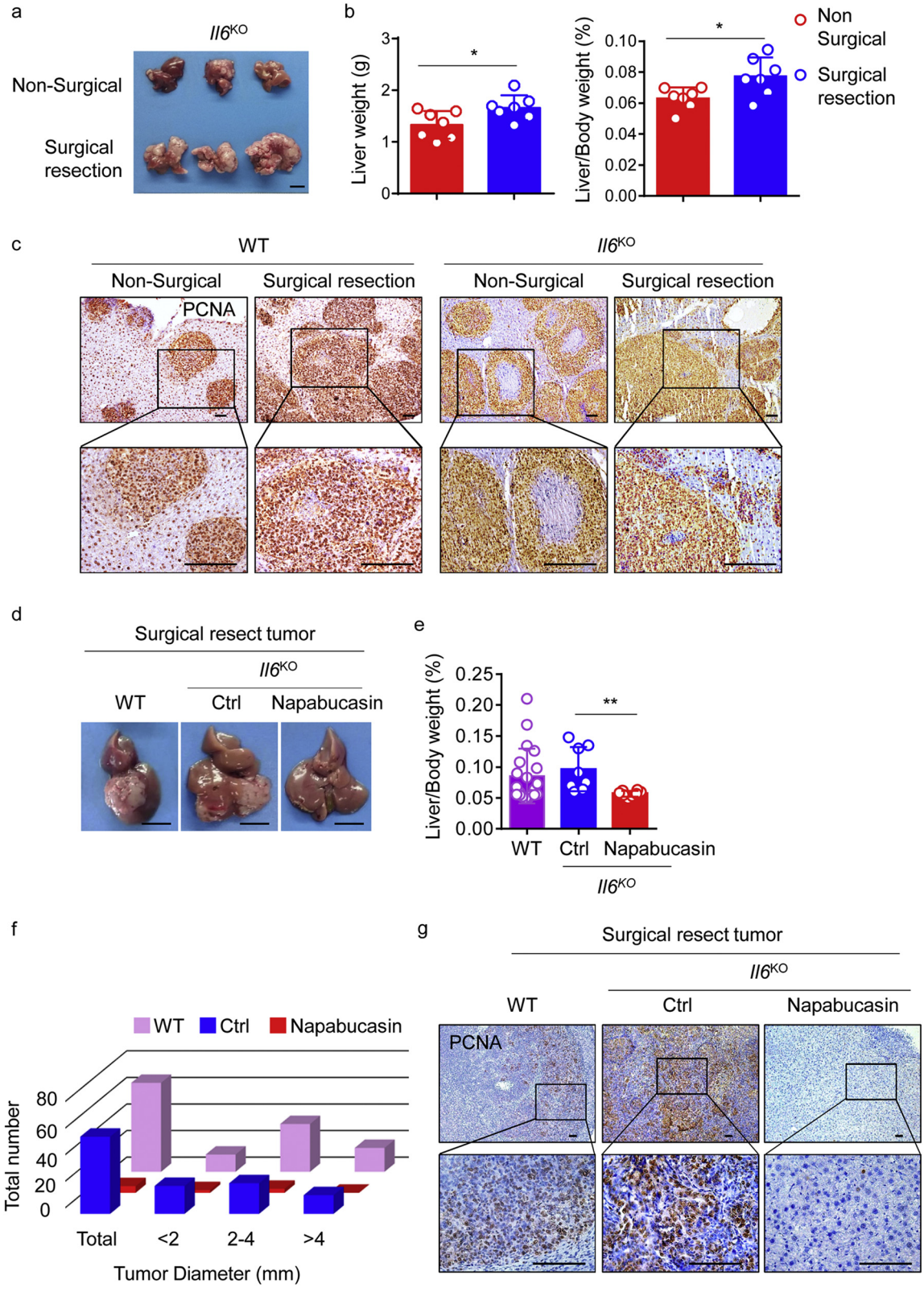

Fig. 7. IL-6 is not required for postsurgical HCC recurrence. (a) Representative picture of HCC in Il6KO mice. A single injection of 1·5 × 106 Hepa1–6 cells was administered to the spleen after the left lateral liver lobe was resected (or not, as a control). Data are representative of three independent experiments, n = 3 per group. (b) HCC burden in individual mice from the non-surgical (red) and surgical resection (blue) groups at autopsy, n = 7 per group. Data are representative of two independent experiments. The results are expressed as mean ± SEM. *p < 0·05 (unpaired Student's t-test). (c) Representative images of PCNA (IHC) staining in tumours from the indicated mice. Data are representative of three independent experiments. Scale bars, 100 μm. (d-f) Representative pictures of HCC samples in which tumour cells were directly injected into the left lateral lobe of the liver in three groups. Middle and right, Il6KO mice after surgical resection of tumours, with (right) or without (middle) napabucasin. Left, WT mouse after surgical tumour resection. Scale bar, 1 cm (d). The ratio of liver weight to body weight was calculated from the indicated groups at autopsy (e). In each mouse, individual tumours were classified according to their size (f). For the images in d and e, data are representative of three independent experiments, n ≥ 8 per group. The results are expressed as mean ± SEM. **p < 0·01 (unpaired Student's t-test). (g) Representative images of PCNA (IHC) staining in the tumour microenvironment in the livers of mice from the indicated groups. Scale bars, 100 μm.

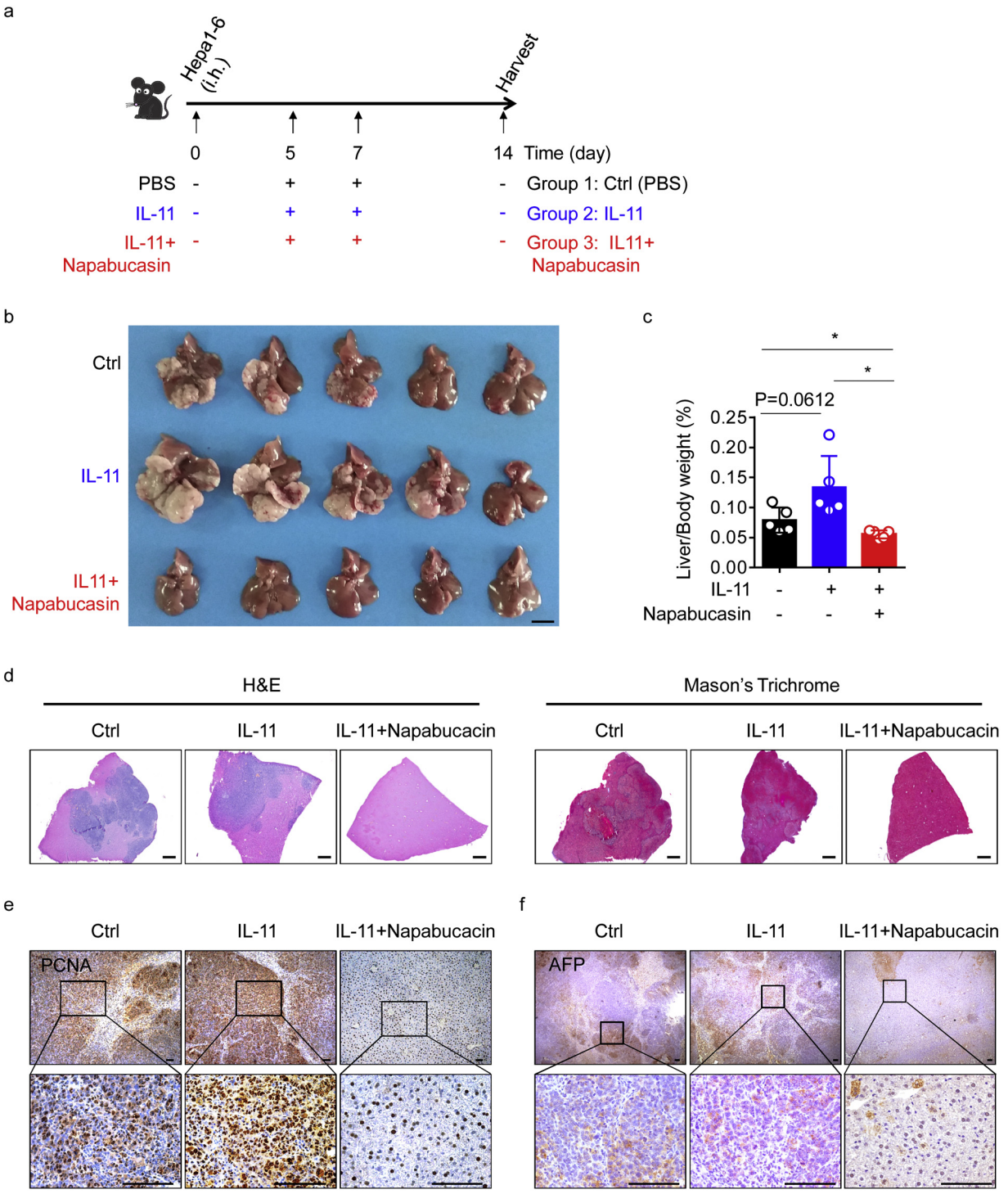

Fig. 8. Napabucasin can prevent IL-11-induced HCC outgrowth *in vivo*. (a) Schematic representation of the HCC model. A single injection of Hepa1–6 cells ($1{\cdot}5 \times 10$ [6]) was administered into the livers of mice, followed by two doses of IL-11 (200 μg/kg) with or without napabucasin (40 mg/kg) on days 5 and 7. (b) Representative pictures of HCC on day 14 from control mice (above), mice treated with IL-11 (middle), and mice treated with IL-11 and napabucasin (below). $n = 5$ for each group. Data are representative of three independent experiments. Scale bar, 1 cm. (c) Ratio of liver weight to body weight calculated for the indicated groups at autopsy. $n = 5$ for each group. The results are expressed as mean ± SEM. $^*p < 0{\cdot}05$ (unpaired Student's *t*-test). (d) Liver damage and fibrosis as assessed by HE and Masson trichrome staining. Scale bars, 400 μm. (e) Representative images of IHC staining of PCNA in tissue sections from the microenvironment of tumours from mice from the indicated groups. Original magnifications: ×10, ×40; scale bars, 100 μm. (f) Representative images of IHC staining of AFP in tissue sections in the tumour microenvironment of tumours from mice from the indicated groups. Original magnifications: ×2·5, ×40; scale bars, 100 μm. For (e) and (f), data are representative of three independent experiments.

4. Discussion

In summary, our current study provides direct evidence that surgery can promote HCC outgrowth and that inhibition of IL-11-STAT3 signaling can effectively prevent postsurgical recurrence. We demonstrated that recurrence is concomitant with regeneration after surgical resection of liver tumours and that elevated IL-11-STAT3 signaling has a key role in inducing tumour outgrowth. Importantly, STAT3 inhibition significantly reduced recurrence. Taken together, our results provide three main insights into the

mechanisms underlying, and potential for prevention of, postsurgical HCC recurrence.

First, we demonstrated HCC recurrence after surgical resection. After reviewing several cancers, we found a high recurrence rate of HCC in various countries. Thus, we used orthotopic tumour, chemically induced genetic mouse, and orthotopic allograft models to reproduce this clinical phenomenon. After surgical resection of liver tumours, we found recurrence in both WT and *Il6*^{KO} mice. As the liver is an organ endowed with regenerative capacity, we wondered whether postsurgical recurrence accompanied regeneration after surgical wounding. Therefore, we constructed surgical wounding models of perforation and hepatectomy. As expected, tumours grew more aggressively in these models than in the sham surgery control. Besides, we found HCC became more aggressive during the regeneration phase, which indicated that surgical resection could simultaneously trigger regeneration and tumour outgrowth. Ablation was also used for the management of HCC [5], and it was reported that the recurrence rate of HCC after ablation was not as high as the recurrence rate after surgery [32,44]. We considered that more tissues were likely to be resected during surgical resection of HCC, and thus might induce a stronger regenerative capacity.

Second, we provide evidence that IL-11-STAT3 signaling has a critical function in HCC outgrowth after surgical resection. Given that recurrence of HCC invariably occurs *in situ* after surgical resection, and that the liver is a central participant in the acute-phase response to systemic inflammation [39], it has been suggested that local, rather than systemic, factors may promote tumour outgrowth in HCC following surgical resection. Using a microarray, we focused on IL-11, which can induce STAT3 activation to promote hepatocyte proliferation and contribute to wound healing [12,17,19]. We found high IL-11 expression levels in tumours, as well as in the livers of mice after surgery. Ernst et al. previously demonstrated that IL-11, rather than IL-6, was the dominant IL-6 family cytokine involved in gastrointestinal tumorigenesis [25,45]. Surprisingly, the outgrowth and postsurgical recurrence of tumours in *Il6*^{KO} mice were similar to those in WT animals; however, tumours were almost completely absent in the *Il-11rα*^{KO} mice after surgical resection, indicating that IL-6 may be less important than IL-11 in HCC recurrence after hepatectomy. Besides, we demonstrated that using siRNA to directly block IL-11-IL-11Rα signaling induced tumour cell apoptosis *in vitro*. Furthermore, we found that IL-11 supplementation induced tumour cell proliferation, and that injection of IL-11 *in vivo* could significantly induce HCC outgrowth in WT mice, with increased expression of PCNA and AFP. This adds to the evidence supporting a critical role for IL-11 signaling in postsurgical recurrence.

Third and finally, we do not propose that tumour resection surgery should be avoided in HCC; instead, we suggest that blocking IL-11-STAT3 signaling would substantially contribute to the prevention of postsurgical recurrence. Numerous therapeutic strategies for cancers have emerged, including targeted drugs and cytokine inhibition; however, there has been less progress in the prevention of recurrence. As our data show that IL-11 has a critical role in HCC outgrowth, and given that excessive STAT3 activation is a characteristic of various solid cancers, we considered whether napabucasin, an inhibitor of STAT3 transcription, could be a useful treatment. Consistent with expectations, napabucasin led to marked death of tumour cells *in vitro*, irrespective of the presence of IL-11. Furthermore, HCC growth was significantly suppressed by napabucasin *in vivo*, regardless of surgery, and this treatment significantly prevented IL-11-induced HCC outgrowth. Of critical importance, experiments using the established surgical orthotopic HCC resection and orthotopic allograft models demonstrated that treatment with napabucasin potently reduced the impact of surgery on HCC recurrence.

Several important questions remain to be explored, mainly relating to the challenges of developing new spontaneous tumour and humanised mouse model systems. For example, we could not determine which cells were the main source of IL-11 after surgical resection, although IL-11 is reported to be partially produced by hepatocytes, with links to compensatory proliferation, upon acute liver injury [38]. Nonetheless, cancer-associated fibroblasts and myeloid cells should not be precluded [12,25]. Nor could we determine the role of the immune system in postsurgical recurrence and regeneration. Notably, myeloid cells can mediate surgery-induced outgrowth of distant tumours in mouse models of dormancy [10], Further, neutrophil extracellular traps can contribute to the awakening of dormant cancer cells during inflammation [46]. Collectively, our results highlight a novel therapeutic strategy and indicate that inhibition of IL-11-STAT3 signaling would help to reduce postsurgical recurrence of HCC.

Funding sources

This work was supported by the Natural Science Foundation of China (# 81788101).

Author contributions

Dongyao Wang designed and conducted experiments, analyzed data, and wrote the manuscript. Xiaohu Zheng and Binqing Fu provided advice. Zhigang Nian conducted some experiments. Yeben Qian helped to collect tissue samples and information from patients. Rui Sun established techniques of flow cytometry and interpreted the data. Zhigang Tian and Haiming Wei designed the study, supervised the research and revised the manuscript.

Declaration of Competing Interest

The authors declare no potential conflict of interest.

Acknowledgments

We thank Mr. Yong Jiang and Ms. Chunxia Ren for their assistance in collecting the specimens involved in this study.

Appendix A. Supplementary data

Supplementary data to this article can be found online at https://doi.org/10.1016/j.ebiom.2019.07.058.

References

[1] Forner A, Reig M, Bruix J. Hepatocellular carcinoma. Lancet 2018;391(10127):1301–14.
[2] Siegel RL, Miller KD, Jemal A. Cancer statistics, 2019. CA Cancer J Clin 2019 Jan;69(1):7–34 [PubMed PMID: 30620402].
[3] Chen W, Zheng R, Baade PD, et al. Cancer statistics in China, 2015. CA Cancer J Clin 2016 Mar-Apr;66(2):115–32 [PubMed PMID: 26808342].
[4] Bray F, Ferlay J, Soerjomataram I, Siegel RL, Torre LA, Jemal A. Global cancer statistics 2018: GLOBOCAN estimates of incidence and mortality worldwide for 36 cancers in 185 countries. CA Cancer J Clin 2018 Nov;68(6):394–424 [PubMed PMID: 30207593].
[5] Hasegawa K, Kokudo N, Makuuchi M, et al. Comparison of resection and ablation for hepatocellular carcinoma: a cohort study based on a Japanese nationwide survey. J Hepatol 2013 Apr;58(4):724–9 [PubMed PMID: 23178708].
[6] Portolani N, Coniglio A, Ghidoni S, et al. Early and late recurrence after liver resection for hepatocellular carcinoma: prognostic and therapeutic implications. Ann Surg 2006 Feb;243(2):229–35 [PubMed PMID: 16432356. Pubmed Central PMCID: 1448919].
[7] Roche B, Coilly A, Duclos-Vallee JC, Samuel D. The impact of treatment of hepatitis C with DAAs on the occurrence of HCC. Liver Int 2018 Feb;38(Suppl. 1):139–45 [PubMed PMID: 29427487].
[8] Grivennikov SI, Greten FR, Karin M. Immunity, inflammation, and cancer. Cell 2010 Mar 19;140(6):883–99 [PubMed PMID: 20303878. Pubmed Central PMCID: 2866629].
[9] Tai LH, de Souza CT, Belanger S, et al. Preventing postoperative metastatic disease by inhibiting surgery-induced dysfunction in natural killer cells. Cancer Res 2013 Jan 1;73(1):97–107 [PubMed PMID: 23090117].
[10] Krall JA, Reinhardt F, Mercury OA, et al. The systemic response to surgery triggers the outgrowth of distant immune-controlled tumors in mouse models of dormancy. Sci Transl Med 2018 Apr 11;10(436) [PubMed PMID: 29643230].
[11] Pound A, McGuire L. Repeated partial hepatectomy as a promoting stimulus for carcinogenic response of liver to nitrosamines in rats. Br J Cancer 1978;37(4):585.

[12] Garbers C, Scheller J. Interleukin-6 and interleukin-11: same same but different. Biol Chem 2013 Sep;394(9):1145–61 [PubMed PMID: 23740659].
[13] Kang S, Tanaka T, Narazaki M, Kishimoto T. Targeting Interleukin-6 Signaling in clinic. Immunity 2019 Apr 16;50(4):1007–23 [PubMed PMID: 30995492].
[14] Wu JB, Yin L, Shi C, et al. MAOA-dependent activation of Shh-IL6-RANKL Signaling network promotes prostate Cancer metastasis by engaging tumor-stromal cell interactions. Cancer Cell 2017 Mar 13;31(3):368–82 [PubMed PMID: 28292438].
[15] Bergmann J, Müller M, Baumann N, et al. IL-6 trans-signaling is essential for the development of hepatocellular carcinoma in mice. Hepatology 2017;65(1):89–103.
[16] Naugler WE, Sakurai T, Kim S, et al. Gender disparity in liver cancer due to sex differences in MyD88-dependent IL-6 production. Science 2007;317(5834):121–4 (New York, NY).
[17] Singh B, Berry JA, Shoher A, Lucci A. COX-2 induces IL-11 production in human breast cancer cells. J Surg Res 2006 Apr;131(2):267–75 [PubMed PMID: 16457848].
[18] Putoczki TL, Ernst M. IL-11 signaling as a therapeutic target for cancer. Immunotherapy-Uk 2015;7(4):441–53 [PubMed PMID: WOS:000353594600010. English].
[19] Xu DH, Zhu Z, Wakefield MR, Xiao H, Bai Q, Fang Y. The role of IL-11 in immunity and cancer. Cancer Lett 2016 Apr 10;373(2):156–63 [PubMed PMID: 26826523].
[20] Li TM, Wu CM, Huang HC, Chou PC, Fong YC, Tang CH. Interleukin-11 increases cell motility and up-regulates intercellular adhesion molecule-1 expression in human chondrosarcoma cells. J Cell Biochem 2012 Nov;113(11):3353–62 [PubMed PMID: 22644863].
[21] Park EJ, Lee JH, Yu G-Y, et al. Dietary and genetic obesity promote liver inflammation and tumorigenesis by enhancing IL-6 and TNF expression. Cell 2010;140(2):197–208.
[22] Sui Q, Zhang J, Sun X, Zhang C, Han Q, Tian Z. NK cells are the crucial antitumor mediators when STAT3-mediated immunosuppression is blocked in hepatocellular carcinoma. J Immunol 2014 Aug 15;193(4):2016–23 [PubMed PMID: 25015826].
[23] Ernst M, Najdovska M, Grail D, et al. STAT3 and STAT1 mediate IL-11–dependent and inflammation-associated gastric tumorigenesis in gp130 receptor mutant mice. J Clin Invest 2008;118(5):1727–38.
[24] Feng T, Dzieran J, Yuan X, et al. Hepatocyte-specific Smad7 deletion accelerates DEN-induced HCC via activation of STAT3 signaling in mice. Oncogenesis 2017 Jan 30;6(1):e294 [PubMed PMID: 28134936. Pubmed Central PMCID: 5294248].
[25] Putoczki TL, Thiem S, Loving A, et al. Interleukin-11 is the dominant IL-6 family cytokine during gastrointestinal tumorigenesis and can be targeted therapeutically. Cancer Cell 2013 Aug 12;24(2):257–71 [PubMed PMID: 23948300].
[26] Fu B, Zhou Y, Ni X, et al. Natural Killer Cells Promote Fetal Development through the Secretion of Growth-Promoting Factors. Immunity 2017 Dec 19;47(6):1100–13 [e6. PubMed PMID: 29262349].
[27] Su XD, Zhang DK, Zhang X, Lin P, Long H, Rong TH. Prognostic factors in patients with recurrence after complete resection of esophageal squamous cell carcinoma. J Thorac Dis 2014 Jul;6(7):949–57 [PubMed PMID: 25093092. Pubmed Central PMCID: 4120168].
[28] Zheng X, Cheng M, Fu B, et al. Targeting LUNX inhibits non-small cell lung cancer growth and metastasis. Cancer Res 2015 Mar 15;75(6):1080–90 [PubMed PMID: 25600649].
[29] Konstantinidis IT, Fong Y. Hepatocellular carcinoma in the modern era: transplantation, ablation, open surgery or minimally invasive surgery? -a multidisciplinary personalized decision. Chin Clin Oncol 2013 Dec;2(4):35 [PubMed PMID: 25841914].
[30] Zhang B, Zhang B, Zhang Z, et al. 42,573 cases of hepatectomy in China: a multicenter retrospective investigation. Sci China Life Sci 2018 Jun;61(6):660–70 [PubMed PMID: 29417360].
[31] Livraghi T, Meloni F, Di Stasi M, et al. Sustained complete response and complications rates after radiofrequency ablation of very early hepatocellular carcinoma in cirrhosis: is resection still the treatment of choice? Hepatology 2008 Jan;47(1):82–9 [PubMed PMID: 18008357].
[32] Yamamoto Y, Ikoma H, Morimura R, Konishi H, Murayama Y, Komatsu S, et al. Optimal duration of the early and late recurrence of hepatocellular carcinoma after hepatectomy. World J Gastroenterol 2015 Jan 28;21(4):1207–15 [PubMed PMID: 25632194. Pubmed Central PMCID: 4306165].
[33] Chen Q, Shu C, Laurence AD, et al. Effect of Huaier granule on recurrence after curative resection of HCC: a multicentre, randomised clinical trial. Gut 2018 Nov;67(11):2006–16 [PubMed PMID: 29802174].
[34] Yang T, Sun YF, Zhang J, et al. Partial hepatectomy for ruptured hepatocellular carcinoma. Br J Surg 2013 Jul;100(8):1071–9 [PubMed PMID: 23754648].
[35] Poon RT-P, Fan S-T, Lo C-M, Liu C-L, Wong J. Intrahepatic recurrence after curative resection of hepatocellular carcinoma: long-term results of treatment and prognostic factors. Ann Surg 1999;229(2):216.
[36] Li X, Yao W, Yuan Y, et al. Targeting of tumour-infiltrating macrophages via CCL2/CCR2 signalling as a therapeutic strategy against hepatocellular carcinoma. Gut 2017 Jan;66(1):157–67 [PubMed PMID: 26452628. [Epub 2015/10/11. eng.].
[37] Cheng X, Wu H, Jin Z, et al. Up-regulation of chemokine receptor CCR4 is associated with human hepatocellular carcinoma malignant behavior. Sci Rep 2017;7(1):12362.
[38] Nishina T, Komazawa-Sakon S, Yanaka S, et al. Interleukin-11 links oxidative stress and compensatory proliferation. Sci Signal 2012 Jan 17;5(207):ra5 [PubMed PMID: 22253262].
[39] Jonker DJ, Nott L, Yoshino T, et al. Napabucasin versus placebo in refractory advanced colorectal cancer: a randomised phase 3 trial. Lancet Gastroenterol Hepatol 2018;3(4):263–70.
[40] Guha P, Gardell J, Darpolor J, et al. STAT3 inhibition induces Bax-dependent apoptosis in liver tumor myeloid-derived suppressor cells. Oncogene 2018 Aug 29;38:533–48 [PubMed PMID: 30158673].
[41] Wan S, Zhao E, Kryczek I, et al. Tumor-associated macrophages produce interleukin 6 and signal via STAT3 to promote expansion of human hepatocellular carcinoma stem cells. Gastroenterology 2014;147(6):1393–404.
[42] Won C, Kim BH, Yi EH, et al. Signal transducer and activator of transcription 3-mediated CD133 up-regulation contributes to promotion of hepatocellular carcinoma. Hepatology 2015;62(4):1160–73.
[43] Li S, Sun R, Chen Y, Wei H, Tian Z. TLR2 limits development of hepatocellular carcinoma by reducing IL18-mediated immunosuppression. Cancer Res 2015 Mar 15;75(6):986–95 [PubMed PMID: 25600646].
[44] Shiina S, Tateishi R, Arano T, et al. Radiofrequency ablation for hepatocellular carcinoma: 10-year outcome and prognostic factors. Am J Gastroenterol 2012 Apr;107(4):569–77 [quiz 78. PubMed PMID: 22158026. Pubmed Central PMCID: 3321437].
[45] Becker C, Fantini MC, Schramm C, et al. TGF-beta suppresses tumor progression in colon cancer by inhibition of IL-6 trans-signaling. Immunity 2004 Oct;21(4):491–501 [PubMed PMID: 15485627].
[46] Albrengues J, Shields MA, Ng D, et al. Neutrophil extracellular traps produced during inflammation awaken dormant cancer cells in mice. Science 2018 Sep 28;361(6409) (New York, NY). [PubMed PMID: 30262472].